Experiments in Fluids 28 (2000) 1–10 © Springer-Verlag 2000

Propeller wake flowfield analysis by means of LDV phase sampling techniques

A. Stella, G. Guj, F. Di Felice

Abstract Two phase sampling techniques are developed for the analysis of the propellers wake by means of LDV. The first one (TTT) uses the detection of Doppler signal as trigger condition; each LDV sample, tagged with the blade angular position at the measurement time, is arranged inside angular slots. The other technique (ATT) follows an angular triggering method, with some enhancements to reduce measurement time. The implemented techniques are complementary from the accuracy and efficiency point of view. The TTT enables to quickly analyze the propellers wake, in view of the minimization of data acquisition time, particularly in poor flow seeding conditions. The ATT is instead suitable for accurate investigations of space-limited and highly turbulent flow regions.

1 Introduction

The accurate experimental investigation of propellers wake flowfield holds an important role in the design and the performance analysis of such propulsion systems. It allows one to both locally check the fulfillment of design requirements, for instance by using the deduced blade sections drag coefficients and bound circulation distribution (Kobayashi 1982; Koyama et al. 1986; Jessup 1989) as well as to get preliminary information for new propeller design. In modern design trend the complexity of blades geometry is increasing, aiming at reducing noise generation, propeller-induced hull ship vibrations, as well as efficiency decay due to cavitation. This aspect has implied a rising interest on measurements of the flowfield around propellers to have a better knowledge of the flow details, particularly for the effects of viscosity and turbulence.

Flow velocity measurements are also important for the validation of existing numerical codes for propeller analysis, based mainly upon potential flow representations and simplified wake models. Nevertheless, a detailed representation of the viscous aspects (Kobayashi 1981), the hub effects (Wang 1985; Blaurock and Lammers 1986) and the actual wake-induced velocity field (Landgrebe and Cheney 1972; Hoshino and Oshima 1987; Pyo and Kinnas 1997) is required for enhancing the accuracy of numerical predictions. The availability of reliable and detailed velocity measurements contributes to fulfill this goal providing guidelines for the development of future models and codes as well as databases for their validation.

The propeller near wake flow presents unsteady velocities with high gradients, strong turbulent fluctuations, hub effects and a three-dimensional pattern. These features require the velocity measurement technique to have adequate performances. Laser Doppler Velocimetry (LDV) is a suitable technique due to its high spatial resolution, good frequency response, velocity direction recognition and, principally, a non-intrusive probe in a such delicate flow. LDV technique has been actually used since seventies for investigating the flow around rotors and propellers both for aeronautical (Landgrebe and Johnson 1974; Biggers and Orloff 1975; Serafini et al. 1981) as well as for marine applications (Min 1978; Kobayashi 1981; Blaurock and Lammers 1986; Cenedese et al. 1984).

In the test section-fixed frame of reference the velocity around a rotating propeller with an axisymmetric inflow varies periodically at a frequency given by the product between the propeller rps and the number of blades. The statistical analysis of the turbulent flow cannot be accomplished through the time averaging of velocity histories acquired in a measurement point. Phase sampling techniques are instead needed in order to execute correct ensemble averaging, referring the velocity field to the propeller angular position. Statistics is based on a large number of propeller revolutions, each one representing an experiment realization.

Received: *29 July 1998*/*Accepted*: *18 February 1999*

A. Stella
Dipartimento di Meccanica ed Aeronautica
Università di Roma "La Sapienza"
Via Eudossiana 18
00184 Rome, Italy
Email: andrea@stella.Ing.Uniromal.it

G. Guj
Dipartimento di Ingegneria Meccanica ed Industriale
Università di Roma Tre, Via della Vasca Navale 79
00146 Rome, Italy
Email: guj@uniroma3.it

F. Di Felice
INSEAN (Italian Naval Basin)
Via di Vallerano 139,
00128 Rome, Italy
Email: f.difelice@mail.insean.it

Correspondence to: G. Guj

The authors would like to express their gratitude to the C.E.I.M.M head Cdr. Elefante and its staff for their precious co-operation. The authors are also grateful to Mr. De Clementi for the realization of the instrument to process the encoder signals, to Dr. Esposito for his contribution in wake measurements graphical visualization.

1.1
Basic approaches to phase sampling acquisition

Two basic approaches can be generally followed to design data acquisition techniques for measuring the phase averaged velocity field around rotors or propellers (Sullivan 1973). The first one is the *time acquisition method*, which envisages the memorization of several time histories of velocity in a space-fixed measurement point, whose peculiar time window is equal to the propeller revolution period T. The second one is the *angular triggering method*, based on the selection of an angular position for which the velocity is acquired once per revolution. The implementation of both the above procedures is not straightforward when the velocity is measured by means of a LDV system. In fact a LDV sample is available only if particles are crossing the measuring volume at the acquisition time. Following the first approach, a certain number of invalid samples can be acquired and unnecessarily stored in the disk. Furthermore, the number of the valid samples could not allow an accurate velocity time history reconstruction. Using the second approach, the velocity measurement may not be obtained due to the lack of a valid LDV sample when propeller reaches the trigger angle. Both methods set therefore stringent demands to LDV data rates and consequently to the level of seeding particles in the fluid. This experimental requirement is yet unpleasant when measurements are performed in a cavitation tunnel, because water conditions invalidate the reliability of propellers cavitation tests.

Techniques based on the time acquisition method have been widely applied, in view of the considerable measurement time saving. Most of these assume the hypothesis of a constant angular velocity of propeller and foresee direct phase sampling of the time-dependent velocity signals basing on the correspondence between time instants and propeller positions (Cenedese et al. 1985; Hoshino and Oshima 1987; Seelhorst et al. 1994; Lammers 1988). In this manner, only one trigger signal per revolution is needed but results uncertainties increases because phase averaging is not relied on the *actual* propeller position. Techniques based on the angular triggering method have been instead rarely used because of the high time consumption and the low efficiency for measuring a such space wide-ranging flow as propeller wake.

1.2
Research goals

The aim of the present research is the development of two LDV phase sampling techniques: the *tracking triggering technique* (TTT) and the *angular triggering technique* (ATT), which follow the two basic approaches but overcoming the limitations caused by a direct implementation. The design is performed with the constraints of poor seeding conditions and without any hypothesis on propeller motion.

In the available LDV system the frequency tracker is used for performing the Doppler signal analysis. Its output is a voltage signal proportional to the Doppler frequency and its mode of operation foresees the holding of the last tracked frequency during the drop out phases. In order to discriminate the tracking phases from those of drop out the TTT and the ATT use the TTL output signal supplied by the tracker (*validation signal* VS), whose high level means the tracking of the Doppler frequency.

In the TTT, the high level of the VS is the triggering event for acquiring LDV samples, which are then tagged with the propeller angular position at the measurement time. During data post-processing, samples collected at a certain radius are arranged along the circumference inside angular slots.

The ATT includes some enhancements to reduce the measurement time with respect to the basic approach. The main improvement is the run time up-to-date of the trigger angle via software, which allows multiple acquisitions during the same propeller revolution.

The implemented techniques are tested and compared measuring the velocity field in the wake of a marine propeller in a cavitation tunnel. The TTT is used to investigate the velocity field and its downstream evolution in the region within the first diameter behind propeller (*near wake*). Some features of the turbulent wake are also pointed out through the calculations of the skewness and the velocity probability functions inside the angular slots. The ATT has been tested measuring a radial profile of the velocity and the Reynolds stresses.

2
Experimental set-up

2.1
Experimental facility and measurement chain

The Italian Navy cavitation tunnel (C.E.I.M.M.) is sketched in Fig. 1. The test section is square, closed jet type, 0.6 m × 0.6 m × 2.6 m. Perspex windows on the four walls enable optical access. The nozzle contraction ratio is 5.96 : 1 and the maximum water speed is 12 m/s. The maximum free stream turbulence intensity in the test section is 2%, which reduces to 0.6% in the propeller blade inflow at 0.7 r/R (being $R = D/2 = 0.117$ m the propeller radius). The flow uniformity is within 1% for the axial component and 3% for the vertical one.

The four blades propeller model (Fig. 2) is skewed, with a uniform pitch to diameter ratio of 1.1 and a forward rake angle of 4°3″. The blockage ratio in the test section is about 10%.

The sketch of the instrumentation set-up is shown in Fig. 3. A 5 mW He–Ne, two channels, reference beam, forward scatter LDV system with trackers is used. The optics are arranged to measure two orthogonal components of velocity simultaneously (V_1, V_2). The TTL validation signals supplied by the

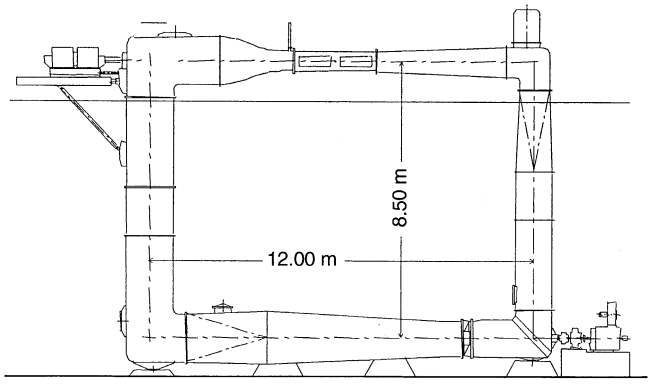

Fig. 1. Italian Navy Cavitation tunnel (C.E.I.M.M.)

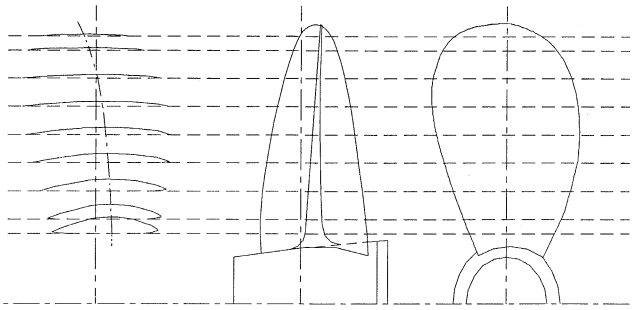

Fig. 2. Tested propeller model

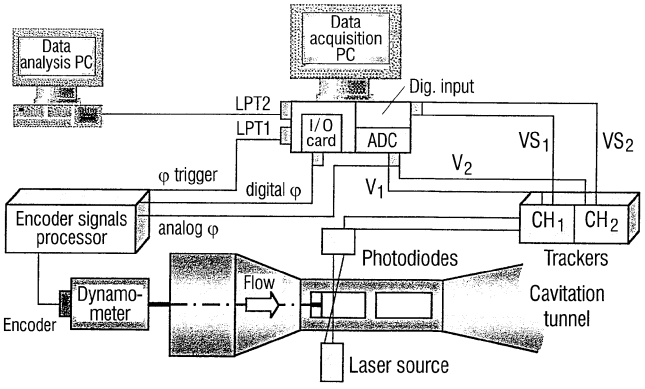

Fig. 3. Schematic representation of the instrumentation set-up

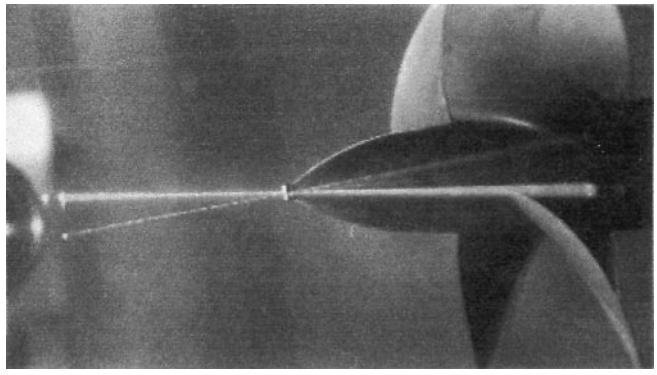

Fig. 4. LDV volume located in the initial reference position by means of a special device

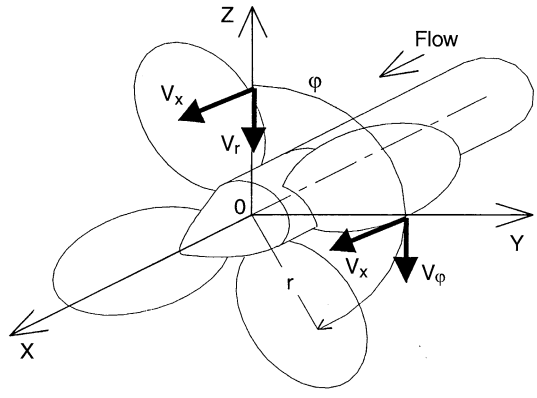

Fig. 5. Co-ordinate systems and measured velocity components

trackers are indicated as VS_1 and VS_2 in the sketch. The LDV measurement volume dimensions are 5.3 and 0.14 mm, in the direction of the optical axis and in the perpendicular one, respectively. Two different measurement campaigns are carried out in order to describe the three-dimensional velocity field using a two-component LDV system. This method requires a high accuracy of LDV probe traversing in the test section as well as of its positioning in the initial reference point to assure that the three components are referred to the same positions. The LDV measurement volume can be traversed with an accuracy of about 0.01 mm. Its initial reference position is fixed by means of a special hub tip, endowed with a hole (shown in Fig. 4), providing an accuracy of 0.5 mm along the optical axis and 0.25 mm in the perpendicular direction. The tunnel water was first filtered and then seeded with 4 μm, spherical particles with high diffraction index. With the adopted seeding levels, the time percentage of the *VS* high ranged within 5–20%, depending on the position of the LDV volume, the level of flow fluctuations and the propeller angular position. The typical tracker input is composed of individual, separated Doppler bursts. A rotary incremental encoder supplies the actual propeller position with an angular resolution of 0.1°. An A/D converter with a resolution of 12 bit, corresponding to a velocity of 2 cm/s, and an input/output card are attached to the acquisition PC as data interfaces.

2.2
Co-ordinate systems and measurement method

A Cartesian O-x, y, z and a cylindrical co-ordinate system O-x, r, φ (Fig. 5) are considered. The LDV system is arranged to measure simultaneously the axial and vertical components of the velocity in the test section fixed frame. In view of the axial symmetry of the propeller inflow and the steady conditions of operation, when the measurement volume is located on the vertical radius (along z-axis), the axial and the vertical components correspond respectively to the axial and the radial ones in the propeller moving frame (Fig. 5). Locating instead the probe in the horizontal radius (y-axis), they represent the axial and the tangential ones. The velocity components in the two co-ordinate systems are related by the standard transformation.

All the measurements in a circumference can be accomplished without moving the LDV volume so that the measurement grid in a plane is obtained by only radial movements. The presence of the hub and model support, which denies optical access to laser beams, does not permit to measure the tangential component between the blade trailing edge and the hub tip.

2.3
Measurement grid and test conditions

The measurement grid (Fig. 6) is constrained by the optical access at $x/R = 0.2$ and wake vortices oscillation amplitude at $x/R = 2.15$. The optical access is limited by the blade passage. The limit in the amplitude of wake vortices oscillations is fixed to the transversal dimension of the tip vortex and determined by preliminary visualizations in cavitating flow conditions.

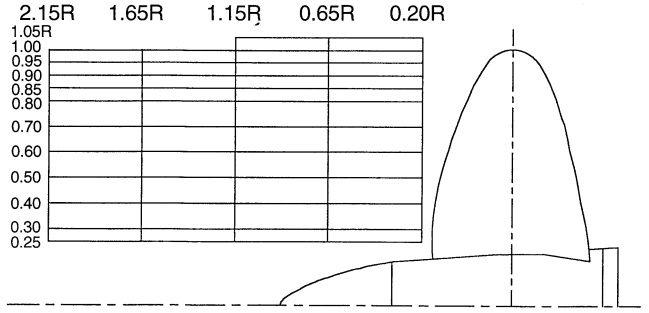

Fig. 6. Map of LDV measurement points in the near wake

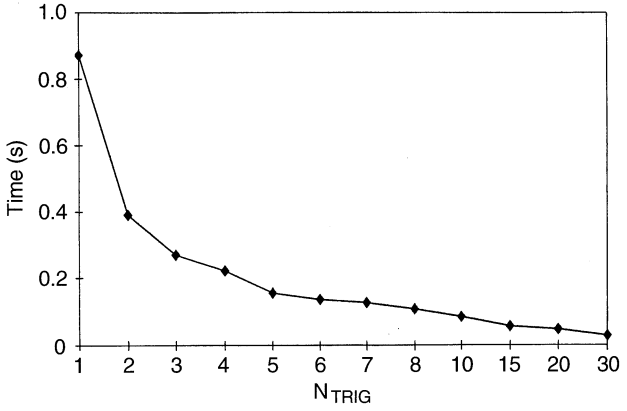

Fig. 7. ATT measurement time versus the number of triggers per revolution

LDV measurements were carried out with a propeller angular velocity $n = 25$ rps and a tunnel water speed $V_\infty = 5$ m/s, giving an advance ratio $J = V_\infty/(\mathrm{n}D)$ of 0.88, near the design value. The blade Reynolds number $Re = (c_{0.7} V_{0.7})/\nu$ is equal to 1.2×10^6, being $c_{0.7}$ the chord length at $r/R = 0.7$ and $V_{0.7} = 13.7$ m/s the relative velocity. A high cavitation number $\sigma_v = (P - P_v)/q = 10.5$, being P the absolute ambient pressure, P_v the vapor pressure and q the stagnation pressure of the propeller upstream flow, is fixed to avoid cavitation development.

3
Phase sampling procedures and data analysis

3.1
Tracking triggering technique (TTT)

Applying the TTT, a velocity sample V_i is acquired when the validation signal VS_i is high. Due to the high Signal to Noise Ratio (SNR) provided by the forward scattering optical configuration and high scattering seeding particles, the VS_i can be considered, in low particle concentration, as Doppler burst detection event. The propeller position is then read with an angular delay of about 0.2° in the test conditions. This TTT acquisition step is repeated independently in the two LDV channels because it was observed that Doppler burst detection is not simultaneous in the two trackers. In post-processing, the sequence of samples relative to a certain radius is arranged inside angular slots of width ε. The sample $V_i(t^*)$, acquired when propeller position was $\varphi(t^*)$, is put in the slot whose center is φ_K, if

$$\varphi_K - \varepsilon/2 < \varphi(t^*) < \varphi_K + \varepsilon/2 \tag{1}$$

The value of ε is chosen to match the maximum of the spatial resolution with statistical requirements.

The TTT characteristics enable to minimize both measurement time and data memorization requirements and are actually advantageous when particles seeding in the fluid is poor and the availability of LDV samples is not time-continuos.

3.2
Angular triggering technique (ATT)

The group of VS_1, V_1, VS_2, V_2 samples are acquired when the actual propeller position reaches a trigger angle φ_{TRIG}. Basing on the value of VS_1 and VS_2, the validation of V_1 and V_2 is then accomplished. Being the propeller revolution period T larger than the time for data reading, validation and storage, the ATT acquisition is repeated during the same propeller revolution, updating the trigger angle via software, as

$$\varphi_{\mathrm{TRIG}}^{i+1} = \varphi_{\mathrm{TRIG}}^{i} + \Delta\varphi_{\mathrm{TRIG}} \tag{2}$$

where $\Delta\varphi_{\mathrm{TRIG}} = 2\pi/N_{\mathrm{TRIG}}$ and N_{TRIG} is the number of triggers per revolution. The ATT time to collect a certain number of samples at a fixed φ_{TRIG} decreases theoretically as $1/N_{\mathrm{TRIG}}$ with increasing N_{TRIG}, until a minimum is reached at N_{TRIGopt}. Figure 7 shows the ATT measurement time evaluated for N_{TRIG} up to 30 ($> N_{\mathrm{TRIGopt}}$).

3.3
Time history technique (THT)

In this technique, which is the implementation of the time acquisition method, the group of VS_1, V_1, VS_2, V_2 samples along with the propeller position are acquired continuously in time until a selected number of samples is reached. The validation of V_1 and V_2 is then executed and validated samples are arranged inside angular slots basing on the propeller position at the measurement time. In the present work, the THT is introduced only for comparison with the TTT and the ATT in terms of measurement efficiency.

3.4
LDV data statistics

The phase averaged velocity field, corresponding to the angular positions φ_K, representing either the slot center using the TTT or the trigger angle applying the ATT, at a fixed radius r and an axial position x, is achieved evaluating the statistical moments of the samples collected at that angle. Considering the i-component of the velocity:

$$V_i(\varphi, t) = V_i(\varphi) + v_i(\varphi, t) \tag{3}$$

the mean value $V_i(\varphi_K)$ is evaluated by the algebraic estimator:

$$V_i(\varphi_K) = \frac{1}{N} \sum_{n=1}^{N} V_{i,n}(\varphi_K) \tag{4}$$

where N is the number of validated samples at φ_K. Analogously, the standard deviation σ_i and the skewness S_i are also calculated through the respective algebraic estimators.

The general time-space correlation between two velocity components $V_i(P_1, t)$ and $V_j(P_2, t+\tau)$, where $P_1=(x_1, r_1, \varphi_1)$ and $P_2=(x_2, r_2, \varphi_2)$, is

$$R_{ij}(OP_1, P_1P_2, t, \tau)=\overline{V_i(OP_1, t)\, V_j(OP_2, t+\tau)} \tag{5}$$

Considering two points located in a circumference, the Eq. (5) becomes

$$R_{ij}\left[(x, r, \varphi_1),(0, 0, \varphi_2-\varphi_1), \frac{\varphi_1}{\varpi}, \frac{\varphi_2-\varphi_1}{\varpi}\right] = \overline{V_i\left[(x, r, \varphi_1), \frac{\varphi_1}{\varpi}\right] V_j\left[(x, r, \varphi_2), \frac{\varphi_2}{\varpi}\right]} \tag{6}$$

The ij component of the Reynolds stresses tensor in P_1 is estimated by the expression:

$$R_{ij}(\varphi_1)=\frac{1}{Q}\sum_{q=1}^{Q} v_{i,q}(\varphi_1)\cdot v_{j,q}(\varphi_1) \tag{7}$$

where Q is the total number of couples of velocities acquired simultaneously in P_1.

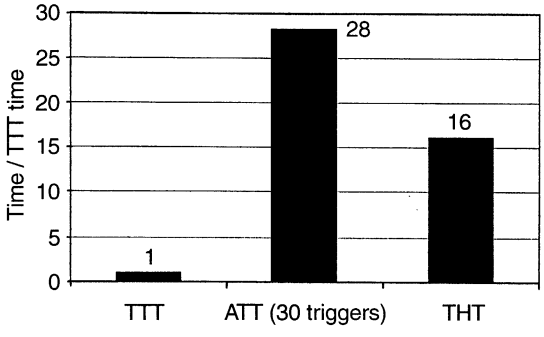

Fig. 8. Time to acquire a valid LDV sample in a certain measurement position

4
Techniques application and wake measurement results

4.1
Efficiency and accuracy of the techniques

The efficiency of the implemented techniques TTT and ATT is evaluated comparing the time to collect a fixed number of valid LDV samples for every angle φ_K along a circumference with that of the THT. Results are shown in Fig. 8. The ATT is tested with $N_{TRIG}=30$, while the acquisition time of the THT is comprehensive of the time for validation and memorization of data in the PC disk. In spite of the dependence of these results on the test conditions (V_∞, n, seeding level, etc.) and on the available apparatus in the measurement chain (e.g. the frequency tracker as Doppler analyzer), some general considerations can be highlighted. Adopting multiple triggers per revolution, the ATT efficiency is comparable with that of the THT, at least in poor seeding conditions. The remarkable time saving using the TTT with respect to the THT is a measure of the advantage, in terms of measurement efficiency, obtained modifying the time acquisition method into this new technique. The advantage increases as the seeding level decreases.

The effect of ε on the TTT velocity profiles can be observed in Fig. 9, where the V_x angular variations corresponding to 1°, 2°, 3° slot widths are compared. The number of samples acquired at the selected radius $r/R=0.7$ is 144.000, corresponding to an average value of 400, 800, 1200 samples for every slot of 1°, 2°, 3° respectively. With $\varepsilon=1°$, the velocity angular variation presents oscillations due to the poor statistics, while with $\varepsilon=2°$ and 3° the profiles are smoother; the blade wake defects for $\varepsilon=1°$ and $\varepsilon=2°$ provide almost the same information, whilst for $\varepsilon=3°$ a spatial filter starts to become effective in the description of the wake velocity defect. In view of these considerations, a slot width of 2° will be adopted.

The distribution inside every slot of samples acquired with the TTT at a fixed r is not uniform but strongly dependent on the angular position of the slot. Figure 10 shows the distribution of 115.200 samples (an average of 640 samples in 180 slots) at $x/R=0.2$, $r/R=0.6$. This profile, which is representative of those occurring at the radii below the tip vortex radial position, is related with the corresponding

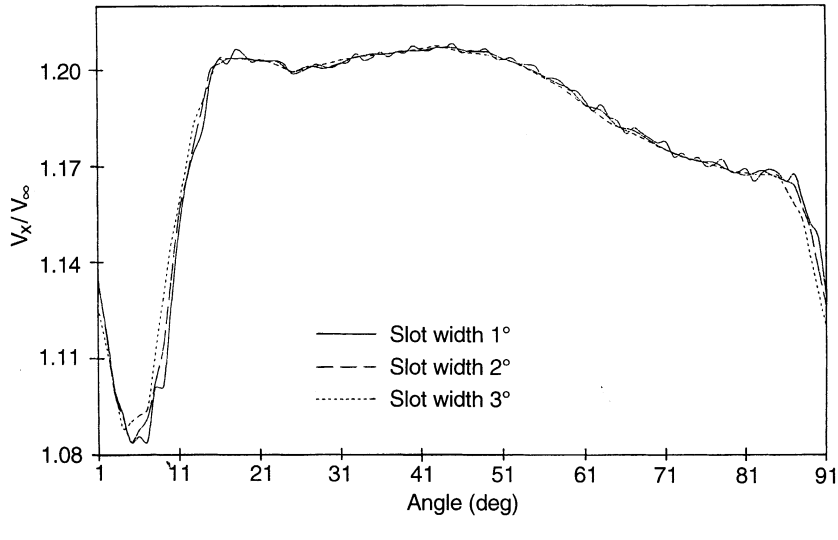

Fig. 9. V_x profile by the TTT with slot width of 1°, 2°, 3°, $X/R=0.2$; $r/R=0.7$

V_x variation. The distribution is formed by four characteristic profiles (as indicated in the figure), periodically oscillating with constant frequency and decreasing amplitude. The formation of these oscillations is explained noting that their period T_{OSC} is equal to the mean time delay $\underline{\Delta t}_{TTT}$ between two consecutive LDV samples acquired by the TTT. The corresponding angular period of such oscillations is $\underline{\Delta\varphi}_{TTT}$ (see Fig. 10). The characteristic oscillating profile begins from the slots located at the blade wake center angles, where a minimum of samples is collected because the flow fluctuations are higher and the fluid seeding is lower, determining a greater probability that tracker drops out. This minimum is then followed by an absolute maximum, located in the slots just beyond the blade wake. The surplus of samples in these slots with respect to the mean value is the compensation of the deficit occurring inside the wake. In fact when a sample is not get in the wake, the first TTT acquisition will occur as soon as the wake is overcame, with growing probability as the flow fluctuations attenuate. The successive oscillations are produced as an effect of translation towards greater angles, with shift $\underline{\Delta\varphi}_{TTT}$, of this trend. The dispersion of the actual Δt_{TTT} values (and consequently of $\Delta\varphi_{TTT}$) around its mean value $\underline{\Delta\varphi}_{TTT}$ during the acquisition produces the gradual damping of the amplitude, introducing a *diffusive* effect on the samples distribution.

Different features are presented by the angular distributions of samples at the same x/R, but for $r/R=0.9$ (tip vortex radius) and $r/R=1.05$ (outside the slipstream), as shown in Fig. 11. At $r/R=0.9$, the distribution is dominated by the effect of the roll-up process, which yields extremely high turbulent flow fluctuations, causing a minimum number of samples in the corresponding slots. Outside the slipstream, the samples distribution does not suffer the periodical effect of the blade passage, since four characteristic trends are not seen. It is randomly oscillating with a much lower dispersion around the mean value of samples for every slot.

A comparison of the accuracy of the ATT and the TTT with $\varepsilon=2^\circ$ in describing the velocity field is proposed in Fig. 12, where the V_x angular variations at $x/R=0.2$, $r/R=0.7$ are shown. Velocity measurements agree very well in the regions far from the blade wake. The ATT better follows the V_x decay due to the blade wake passage and proves, in general, to be more effective for measuring in regions of highly turbulent flow. Such difference is ascribed to the lack or the lower number of triggers during data acquisition using the TTT,

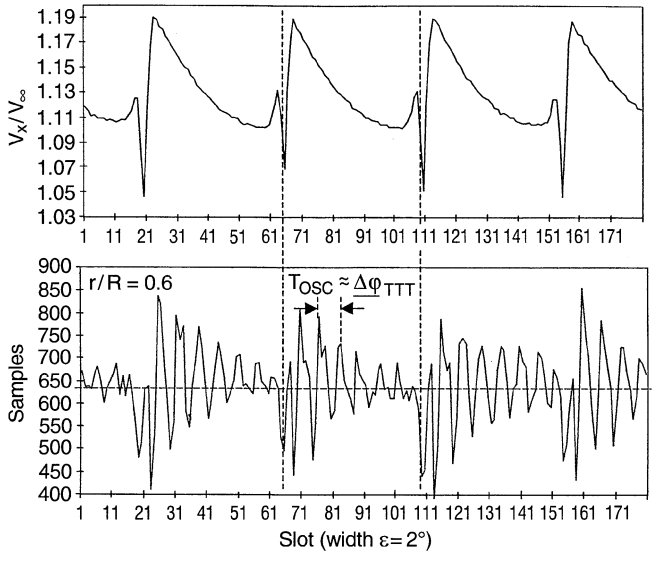

Fig. 10. Distribution of TTT samples versus the slot angular position with related V_x profile $X/R=0.2$, $r/R=0.6$

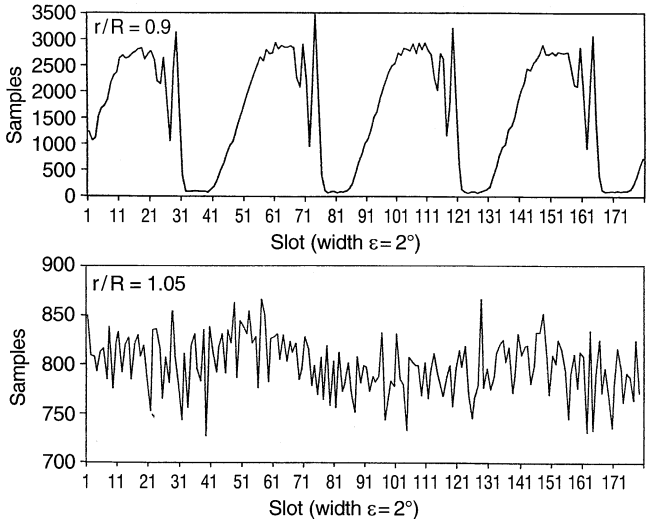

Fig. 11. Distribution of TTT samples versus slot angular position. $X/R=0.2$, $r/R=0.9$ and $r/R=1.05$

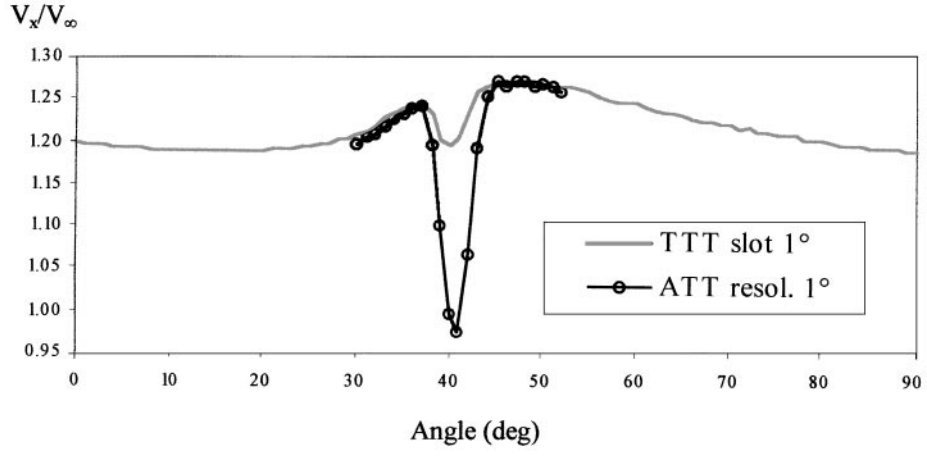

Fig. 12. Comparison of the V_x profile in the blade wake obtained by the ATT and the TTT $X/R=0.2$, $r/R=0.7$

either in those angles where or at those instants when the flow fluctuations are the highest. This occurs because the tracker either drops out in such flow conditions or it supplies a too short tracking time window (that is the duration of the VS_i TTL signal high), to be detected by the available hardware. The ATT is instead less influenced by the length of the tracking time, providing that it is not systematically null, because the trigger condition is unfailingly given once per revolution and the acquisition lasts until a selected number of valid samples is reached at a considered triggering angle. On the other hand, the TTT acquisition stops if a total number of samples is collected at a fixed radius, without assuring that a selected number is get at a particular angle and in any case with greater probability to acquire samples where/when flow is less turbulent.

4.2
Near wake analysis using the TTT

The high efficiency of the TTT allows one to rapidly investigate wide regions of the propeller wake with a high spatial resolution. Some outlines of TTT results will be presented in the following, while more details are provided by Stella et al. (1998).

Figure 13 shows the V_x and σ_x distributions on the measurement planes. The passage of the blade *viscous wake*, produced by the boundary layers on the blade surfaces joining at the trailing edge, is indicated by defects of the V_x. At the blade root deeper V_x defects are measured and a neighboring region of slow flow, which extends in the pressure side of the blade, can be also noticed. This flow distribution in the inner radii is due to the increasing thickness of the blade sections toward the root, as well as to the fact that the LDV measurement points are closer to the blade trailing edge. The strong gradients and the V_x peak at $r/R = 0.9$ are generated by the presence of the tip vortex. The highest axial flow accelerations and the thinnest viscous wake deficits along the blade wake occur around $r/R = 0.7$, meaning that the corresponding blade sections are the most efficient for propeller thrust generation.

The σ_x distribution enables to point out very well the shape of the blade wake and the tip vortex core movement toward the suction side, which causes an abrupt curling at the tip. The maximum value of the σ_x/V_∞ at the trailing edge measurement plane is about 20% in the tip vortex core. Along the blade wake, the highest axial fluctuations are measured at the root sections, with $\sigma_x/V_\infty = 10 \div 14\%$, while σ_x has a minimum around $r/R = 0.7$. The effects of the propeller hub can be described in a certain detail: its boundary layer causes an irregularly bounded region of high σ_x around the hub, with radial peaks spreading outwards. Far from the hub and the blade wake, σ_x/V_∞ reaches the level of the free stream (2%).

Near wake geometry is characterized by a strong deformation process due to the progressive bending of the blade wake surfaces, induced by the cross flow, and the tip vortex trajectory. The slipstream contraction is marked just behind the propeller and is practically complete within the first diameter. The cross velocity field in the fixed frame and the axial component of the vorticity ϖ_x at $X/R = 1.15$ are sketched in Fig. 14. The *trailing vorticity* (*potential wake*), shed from the blade trailing edge, which is modeled with no thickness according to a potential theory, is instead actually widespread over a finite thickness as an effect of the viscous and turbulent diffusion.

A deeper analysis of the turbulent wake at the trailing edge is accomplished evaluating the probability of V_x (P_x) and the skewness S_x inside the slots. The S_x angular variations (Fig. 15a) in the blade wake is generally negative, with two peaks located besides the turbulent wake center, (which in this work is defined as the angular position where σ_x is maximum). Considering a P_x in the suction side of the blade wake (Fig. 15b), an asymmetrical profile can be noticed due to the presence of samples corresponding to a slower axial flow. This shape reveals the presence of blade wake unsteadiness and local flow separations and is associated with minimum S_x. The low value of the S_x modulus in the wake center indicates a less unsteady flow and more symmetrical P_x. Far from the blade wake, both inside ($r/R = 0.7$, Fig. 15c) and outside ($r/R = 1.05$, Fig. 15d) the slipstream, the P_x are symmetrical and identical to those of the free stream in the test section. This result confirms that turbulence in these regions is due to the upstream flow and not produced by the propeller.

4.3
Local detailed measurements by the ATT

The ATT features of (i) high accuracy measuring in regions of highly turbulent flow and strong velocity gradients, (ii) allowing the control of the angular position of a LDV sample, jointly with (iii) the measurement time saving provided by executing multiple acquisitions per revolution make this technique suitable to earn complementary information in space-limited wake flow regions, such as blade wake, tip vortex, hub flow. This is particularly important for the purpose of executing quantitative measurements of the Reynolds stresses R_{ij}. In this case the ATT provides accurate samples of two velocity components referred to the same angle φ_1 and acquired at same instant according to Eq. (7). The R_{xx}, R_{xr} and R_{rr} at $X/R = 0.2$, $r/R = 0.7$, corresponding to an angular position within the blade wake and to another one far from the blade flow are presented in Fig. 16a and Fig. 16b respectively. 200 samples are collected for each angle. In both cases, R_{xx} and R_{rr} are dominant with respect to the cross component R_{xr}. The blade wake turbulence produces Reynolds stresses 2 orders of magnitude larger than the ones of the undisturbed flow, where R_{xr} is practically null.

5
Final remarks and conclusions

Results of the application of two LDV phase sampling techniques for the analysis of a marine propeller wake flowfield in a cavitation tunnel were presented. The techniques are developed with the fluid poorly seeded, using a frequency tracker as Doppler signal analyzer and without any hypothesis on the propeller motion, relying phase sampling on the actual propeller position.

Using the TTT, a technique based on a modified time acquisition method, where the triggering event is the detection of Doppler signal and LDV samples are arranged inside angular slots, a high measurement efficiency can be obtained also in poor seeding conditions. This technique as well as the other, presently applied to the tracker processor, can be

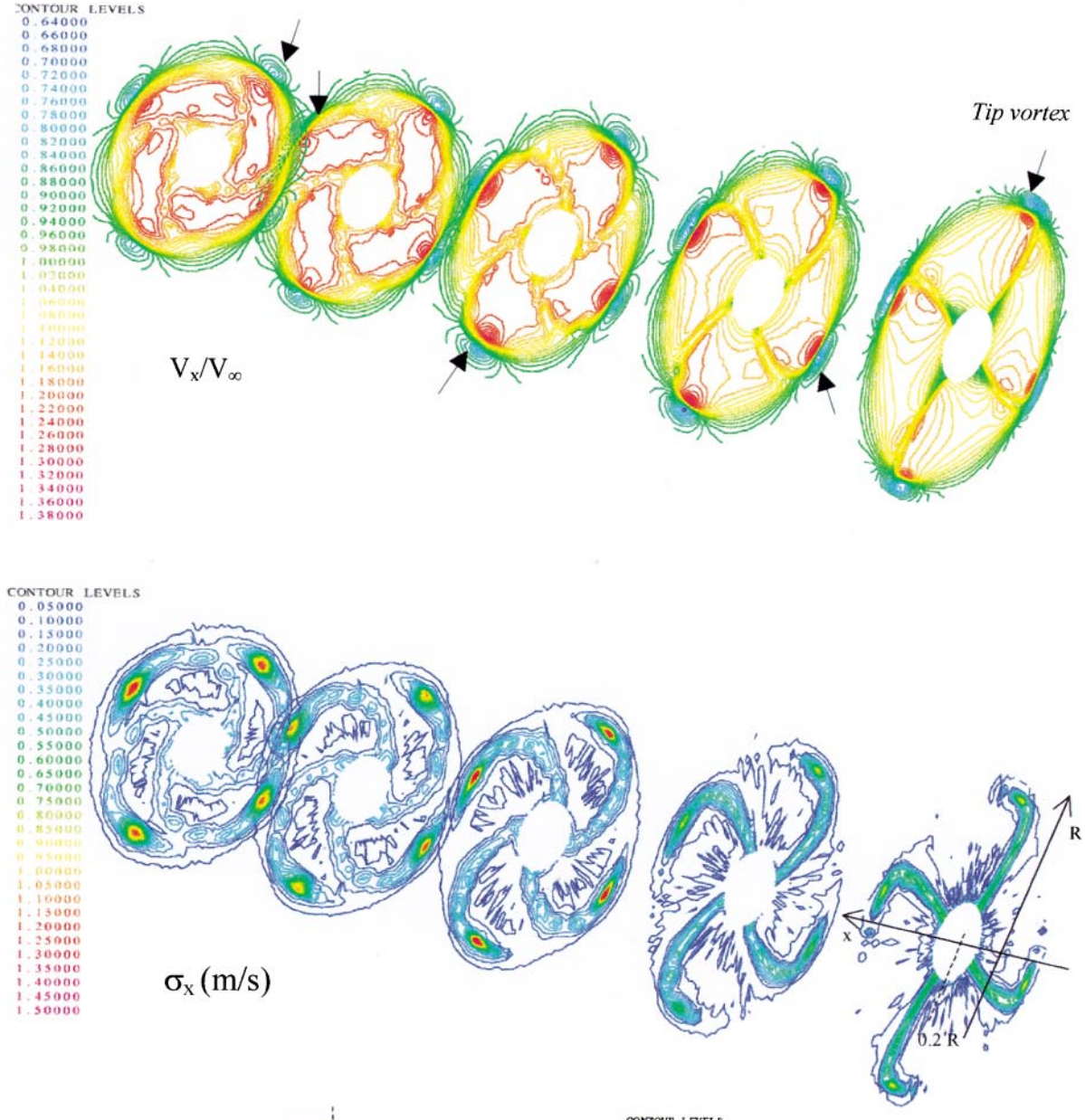
CONTOUR LEVELS
0.64000
0.66000
0.68000
0.70000
0.72000
0.74000
0.76000
0.78000
0.80000
0.82000
0.84000
0.86000
0.88000
0.90000
0.92000
0.94000
0.96000
0.98000
1.00000
1.02000
1.04000
1.06000
1.08000
1.10000
1.12000
1.14000
1.16000
1.18000
1.20000
1.22000
1.24000
1.26000
1.28000
1.30000
1.32000
1.34000
1.36000
1.38000
Tip vortex
V_x/V_∞
CONTOUR LEVELS
0.05000
0.10000
0.15000
0.20000
0.25000
0.30000
0.35000
0.40000
0.45000
0.50000
0.55000
0.60000
0.65000
0.70000
0.75000
0.80000
0.85000
0.90000
0.95000
1.00000
1.05000
1.10000
1.15000
1.20000
1.25000
1.30000
1.35000
1.40000
1.45000
1.50000
σ_x (m/s)
R
x
0.2 R

Fig. 13

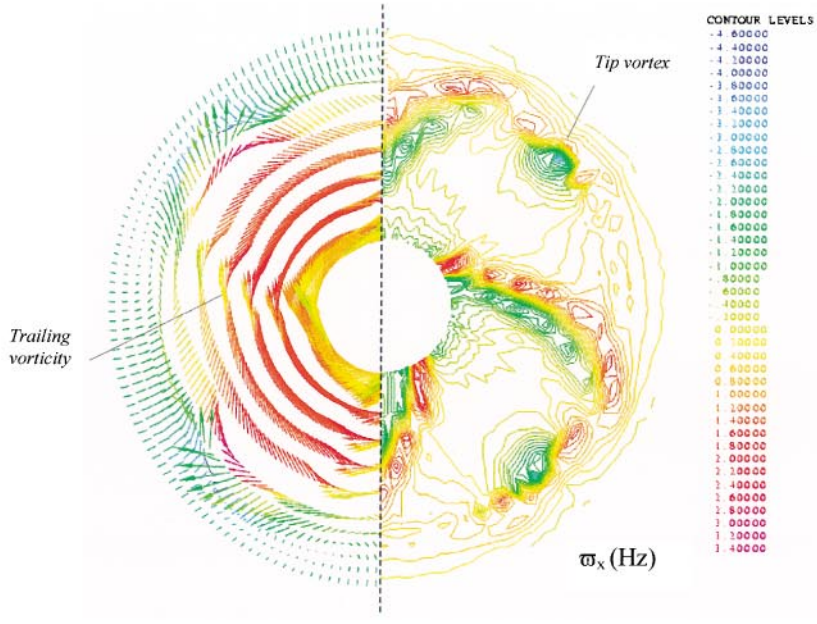
Tip vortex
Trailing vorticity
ϖ_x (Hz)
CONTOUR LEVELS
-4.60000
-4.40000
-4.20000
-4.00000
-3.80000
-3.60000
-3.40000
-3.20000
-3.00000
-2.80000
-2.60000
-2.40000
-2.20000
-2.00000
-1.80000
-1.60000
-1.40000
-1.20000
-1.00000
-.80000
-.60000
-.40000
-.20000
0.00000
0.20000
0.40000
0.60000
0.80000
1.00000
1.20000
1.40000
1.60000
1.80000
2.00000
2.20000
2.40000
2.60000
2.80000
3.00000
3.20000
3.40000

Fig. 14

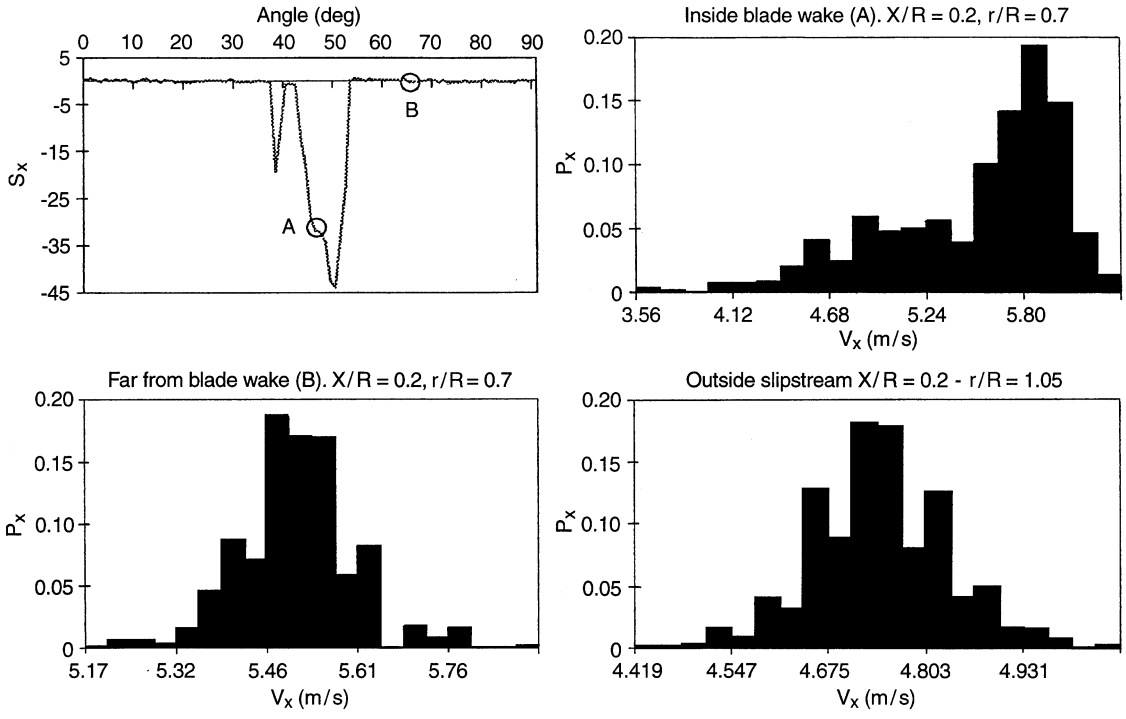

Fig. 15. $X/R = 0.2$, $r/R = 0.7$. (**a**) Skewness angular variation; (**b**) P_x inside blade wake (point A); (**c**) P_x far from the blade wake (point B); (**d**) $X/R = 0.2$, $r/R = 1.05$. PDF outside the slipstream

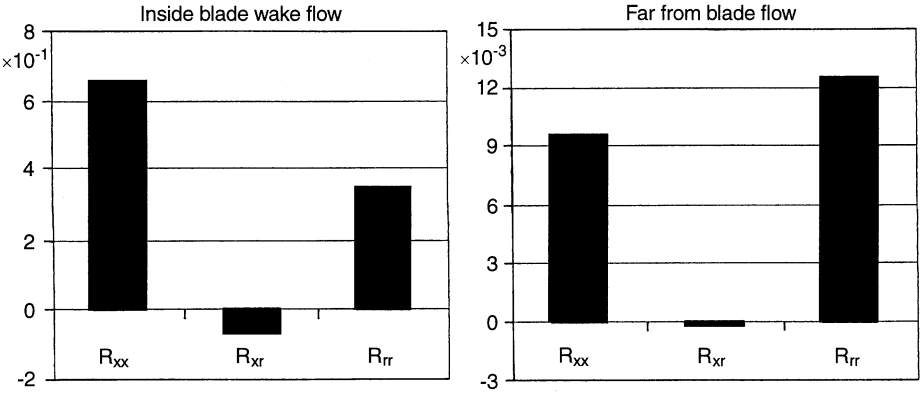

Fig. 16. Reynolds stresses by the ATT. $X/R = 0.2$, $r/R = 0.7$; (**a**) Inside blade wake; (**b**) Far from blade wake

generalized to any other type of Doppler processor having the capability to provide a synchronization signal when a validate measurement is obtained. The TTT proves to be suitable for routine analyses of the propeller wake and some outlines of results have been presented, highlighting the ability to characterize the viscous, the potential and the turbulent wakes and their downstream evolution.

The proposed angular triggering technique (ATT) performs multiple acquisition per revolution allowing a considerable measurement time saving with respect to the basic approach and provides high accuracy in regions of high fluctuating flow and strong velocity gradients. The ATT proves to be suitable to focus the analysis on space-limited wake regions, such as blade wake, tip vortex and hub flow. Results of ATT application to describe the velocity variation within the blade wake and to calculate the Reynolds stresses have been presented.

The implemented phase sampling techniques result thus complementary from the accuracy and efficiency point of view, allowing one to face the experimental analysis of the propeller wake flowfield with effective and several purposes means of investigation.

Fig. 13. Axial mean velocity and standard deviation distribution in the measurement planes at $X/R = 0.2$, 0.65, 1.15, 1.65, 2.15

Fig. 14. Cross flow velocity field in the fixed frame and axial component of the vorticity ϖ_x. $X/R = 1.15$

References

Biggers JC; Orloff KL (1975) Measurements of the helicopter rotor-induced flow field. J Amer Helicopter Soc 20: no. 1 July

Blaurock J; Lammers G (1986) Measurements of the time-dependent velocity field surrounding a model propeller in uniform water flow. Proc. of the Symposium on Aerodynamic and Related Hydrodynamic Studies Using Water Facilities, Monterey, California – AGARD, paper No. 30

Cenedese A; Accardo L; Cioffi F (1984) Experimental analysis of tip vortex by laser-Doppler anemometry. Proc II Int Conf on Application of laser-Doppler Anemometry to Fluid mechanics, Lisbon

Cenedese A; Accardo L; Milone R (1985) Phase sampling techniques in the analysis of a propeller wake. Proc Int Conf on Laser Anemometry Advances and Application, Manchester (UK)

Hoshino T; Oshima A (1987) Measurement of flow field around propeller by using a 3-component laser Doppler velocimeter. Mitsubishi Technical Review, 24: 46–53 method. J Soc Naval Architects Japan

Jessup SD (1989) An experimental investigation of viscous aspects of propeller blade flow. PhD Thesis. The Catholic University of America, Washington DC

Kobayashi S (1981) Experimental methods for the prediction of the effects of viscosity on propeller performance. Dept. of Ocean Engineering, Rep. 81-7 MIT

Kobayashi S. (1982) Propeller wake survey by laser Doppler velocimeter. Proc. of the International Symposium on the Application of laser-Doppler Anemometry to Fluid mechanics, Lisbon

Koyama K; Kagugawa A; Okamoto M (1986) Experimental investigation of flow around a marine propeller and application of panel method to the propeller theory, Proc. of the 16th Symposium on Naval Hydrodynamics

Lammers G (1988) LDA measurements of the tip vortex velocity field in the slipstream of model propellers. Proc 4th International Symposium on Application of Laser Anemometry to Fluid Mechanics, Lisbon

Landgrebe AJ; Cheney MC (1972) Rotor wakes – key to performance predictions. AGARD, CP 111

Landgrebe AJ; Johnson BV (1974) Measurement of model helicopter rotor flow velocities with a laser Doppler velocimeter. J Amer Helicopter Soc 19: no. 3 July

Min KS (1978) Numerical and experimental methods for prediction of field point velocities around propeller blades. Dept. of Ocean Engineering, Report no. 78-12, MIT

Pyo S; Kinnas SA (1997) Propeller wake sheet roll-up modeling in three dimensions. J Ship Res 41: 81–92

Seelhorst U; Beensten BMJ; Butefisch KA (1994) Flow field investigation of a rotating helicopter rotor blade by three-component laser Doppler velocimetry. AGARD CP 55

Serafini JS; Sullivan JP; Neumann HE (1981) Laser Doppler flow-field measurements of an advanced turboprop, 17th Joint Propulsion Conference, AIAA/SAE/ASME, Colorado Springs, Colorado

Stella A; Guj G; Di Felice F; Elefante M(1998) Propeller wake evolution analysis by LDV. Proc 22nd Symp on Naval Hydrodynamics, Washington, DC

Sullivan (1973) An experimental investigation of vortex rings and helicopter rotor wakes using a laser Doppler velocimeter. MIT, AD-778768

Wang MH (1985) Hub effects in propeller design and analysis. Dept. of Ocean Engineering Rep. 85-14, MIT